Composites: Part A 43 (2012) 1285–1292

Contents lists available at SciVerse ScienceDirect

Composites: Part A

journal homepage: www.elsevier.com/locate/compositesa

Monitoring the mechanical behavior under ramp and creep conditions of electrically conductive polymer composites

D. Pedrazzoli, A. Dorigato *, A. Pegoretti

University of Trento, Department of Materials Engineering and Industrial Technologies and INSTM Research Unit, Via Mesiano 77, 38123 Trento, Italy

ARTICLE INFO

Article history:
Received 25 October 2011
Received in revised form 22 March 2012
Accepted 25 March 2012
Available online 5 April 2012

Keywords:
A. Polymer–matrix composites (PMCs)
B. Creep
C. Damage mechanics
D. Mechanical testing

ABSTRACT

In this work a nanomodified epoxy matrix was used to prepare glass fibers reinforced laminates to be tested under ramp and creep conditions, with a continuous monitoring of their deformational and damage behavior through electrical measurements. A combination of carbon black (CB) and carbon nanofibers (CNFs), with a relative CB/CNF ratio of 90/10 and a total filler amount of 2 wt.%, was selected to prepare nanomodified composite laminates by a hand lay-up technique. Tensile tests under ramp and creep conditions highlighted a remarkable strain and damage monitoring capability of the prepared composites, with a strong dependency of the response on the testing temperature and on the load level.

1. Introduction

Fiber reinforced polymers (FRPs) are structural materials, specifically designed for lightweight constructions, for which extremely high mechanical performances are generally expected [1].

Due to their high specific mechanical properties under short-term (ramp loading) and long-term (creep and fatigue) loading conditions, FRPs find an increasing application in the design of structural components, for which the retention of elevated performances for an extended lifetime is required.

Since the breakage of composite structures often occurs by interfacial delamination and/or matrix cracking, the investigation of reliable methods for the failure detection in FRPs has recently attracted the interest of both the scientific and industrial community. Therefore, experimental techniques for the in situ monitoring of the strain and/or damage behavior of composite structures could represent an important aspect to increase their reliability. Both traditional methods (based on the application of strain gauges and piezoelectrics) and innovative monitoring techniques (i.e. through fiber optics) usually make use of sensors that, placed either inside or outside the structure, are invasive and relatively expensive [2]. In order to overcome such drawbacks alternative monitoring systems, based on the intrinsic conductive properties of specifically developed materials has been recently proposed [3]. This methodology implies the measurement of the electrical resistance of the components, without any additional sensors. Due to the rather good electrical conductivity of carbon fibers, monitoring methods based on electrical conductivity have been widely investigated for the failure detection in carbon fiber reinforced polymers (CFRPs) [4–6]. The usage of an electrically conductive polymer matrix can provide some insight on matrix-related failure mechanisms eventually enabling the approach also for structural composites reinforced with non conductive fibers, such as glass, basalt or organic fibers.

The damage detection in composite parts through matrix conductivity measurements offers several advantages compared to traditional optical fibers sensors. In fact, the reliability of these sensors for damage detection in large composite parts is not satisfactory for various reasons. For instance, due to their elevated cost it is not possible to apply a dense network of optical glass fibers to large composite components, and if a crack is propagating without crossing one of the sensors the damage would not be detected. Moreover, in some cases thick optical fibers may also be a source of damage initiation when inserted in composite parts [7,8].

Thanks to their low density and their good adhesive and mechanical properties, epoxy resins are the most diffuse matrices for structural composites. Furthermore, it has been widely proven that the introduction of small amounts of nanostructured materials in epoxy matrices can substantially increase their mechanical properties [9–16] and thermal stability [17,18]. Furthermore, it has been proven how the addition of metal and carbon based nanofillers, such as metal nanopowders, graphite nanoplatelets (GnPs), carbon black (CB) and carbon nanofibers (CNFs) could dramatically enhance the electrical conductivity of the resulting materials [19–24]. The electrical behavior of these filled systems can be successfully described referring to the percolation theory [25]. After a given filler content,

* Corresponding author. Tel.: +39 0461 282412; fax: +39 0461 281977.
E-mail address: andrea.dorigato@ing.unitn.it (A. Dorigato).

1359-835X/$ - see front matter © 2012 Elsevier Ltd. All rights reserved.
http://dx.doi.org/10.1016/j.compositesa.2012.03.019

the so-called percolation threshold, the conductive particles form a continuous network through the insulating matrix and the resistivity drastically decreases by several orders of magnitude.

Some attempts have been recently made to prepare composite laminates in which the epoxy matrix was nanomodified with conductive nanofillers. For instance, Thostenson and Chou [26] reported the preparation of carbon nanotube (CNT) modified epoxy-glass fiber composites, investigating their strain and damage sensing capability. It was shown that with a CNT concentration of 0.5 wt.% within the epoxy matrix, quasi-static behavior as well as matrix failure could be effectively detected by electrical conductivity measurements. With the same technique, Boeger et al. [27] monitored the fatigue behavior and the interlaminar shear strength of glass fiber reinforced composites, in which the matrix was modified with CNT and CB nanoparticles in order to achieve an elevated electrical conductivity. Also Kostopoulos et al. [28] investigated the fatigue monitoring of carbon fiber reinforced laminates, by using an epoxy matrix nanomodified with CNT. Nanni et al. [29] studied the self-monitoring capability of glass fiber reinforced composite rods, constituted by an inner conductive core and an external structural skin, performing both tensile and fatigue tests. In that case the electrical conductivity of the inner core was enhanced through the addition of CB nanoparticles having different surface area. It was found that filler dispersion was the key feature affecting the self-monitoring behavior of the prepared materials, and only high surface area nanoparticles could ensure an adequate self-monitoring reliability.

Quite surprisingly, to the best of our knowledge, no papers dealing with the electrical monitoring of nanofilled FRPs under creep conditions can be found in the open scientific literature. In a previous work of this research group [30] it has been reported how the introduction of a proper combination of carbon black and carbon nanofibers in an epoxy matrix could lead to a remarkable increase of its bulk conductivity values. Furthermore, it was also demonstrated that both the strain and the failure induced by the application of ramp and creep loads could be effectively detected in these nanocomposites through rather simple electrical conductivity measurements. Therefore, the aim of this work is to investigate the potential of such nanocomposite epoxy resin, to be used as a matrix in glass fiber reinforced laminates whose strain and damage evolution under ramp and creep loading conditions is monitored by electrical resistivity measurements.

2. Experimental section

2.1. Materials and sample preparation

A bicomponent epoxy resin, supplied by Elantas Camattini SpA (Collecchio, Italy), was selected. In particular, EC157 epoxy base (density = 1.15 g cm^{-3}, viscosity = 700 mPa s), constituted by a mixture of Bisphenol A/Bisphenol F/Hexanediol diglycidyl ether (equivalent epoxide weight (EEW) = 165–180 g $equiv^{-1}$), was added to W152 LR amminic hardener (density = 0.95 g cm^{-3}, viscosity = 30 mPa s) at a weight ratio of 100:30.

Carbon black nanoparticles (Ketjenblack EC600JD) were provided by Akzo Nobel Chemicals SpA (Arese, Italy). This nanofiller is characterized by fine aggregates of spherical primary particles with a mean size of around 30 nm (specific surface area = 1353 - m^2 g^{-1}, density of 1.95 g cm^{-3}). Vapor grown carbon nanofibers (1195 JN) have been supplied by NanoAmor Inc. (Houston, USA). These nanofibers have a length of 5–40 μm, a core diameter of 0.5–10 nm and an outside diameter of 240–500 nm (specific surface area = 29 m^2 g^{-1}, density of 1.78 g cm^{-3}).

Balanced E glass woven fabrics having an areal density of 200 g m^{-2} were supplied by URS Schaller Sas (Firenze, Italy). All materials were used as received.

The epoxy base, the hardener and the selected amount of nanofiller were dosed in a beaker and manually mixed for 5 min. The mixture was then mechanically stirred for 5 min at 2000 rpm in a Dispermat® F1 mixer followed by a degassing stage under vacuum for 10 min. A six layers laminate of 30 × 30 cm^2, sealed on both sides with Mylar® sheets, was prepared by a wet hand lay-up process and subsequently pressed at 1 MPa in a Carver (Wabash, USA) laboratory press. The hot pressing was carried out at 50 °C for 2 h and at 100 °C for the following 2 h, with degassing during the first 10 min. This thermal treatment was selected in order to speed up the preparation of the samples without affecting the final properties of the cured resin. Composite laminates based on neat epoxy resin were prepared in the same way and their final thickness was in the range 0.7–0.9 mm. The specimens were cut out from the composite laminates using a high speed disk cutter.

In the first part of this research [30] the thermo-mechanical properties and the electrical monitoring capability under ramp and creep conditions of the epoxy matrix nanomodified with different amounts of CB and CNF was investigated. In particular, the nanocomposite matrix with a total nanofiller content of 2 wt.% and a CB/CNF ratio of 90/10 emerged as the best compromise between the electrical behavior (resistivity values of 10^3–10^4 Ω cm) and the mechanical properties (18% increase of the elastic modulus with respect to the neat matrix).

Therefore, in the present paper this matrix composition was selected for the preparation of composite laminates. The notation Epoxy-GF indicates the composite prepared by using the neat epoxy, while Epoxy-CB/CNF-90/10-2-GF refers to the nanomodified laminate with a total nanofiller content of 2 wt.% and a CB/CNF weight ratio of 90/10.

2.2. Experimental techniques

2.2.1. Thermo-gravimetric and microstructural characterization

Density measurements were performed through a Micrometrics AccuPyc 1330 helium pycnometer at 23 °C by using a cell volume of 3.5 cm^3, while thermogravimetric analysis (TGA) were carried out through a Mettler TG 50 thermobalance (Schwerzenbach, Switzerland). The information of these analyses were combined in order to determine the relative concentration of the constituents in the laminates. TGA were carried out imposing a temperature ramp between 40 and 800 °C at a heating rate of 10 °C min^{-1} by using an air flow of 200 ml min^{-1}. Fiber volume fraction (Φ_f) in the laminates was assessed as:

$$\Phi_f = \frac{\rho_{comp}}{\rho_f} W_f \tag{1}$$

where W_f is the weight fiber fraction obtained from the TGA test, while ρ_{comp} and ρ_f denote the density of the composite and of the fiber, respectively. As indicated in ASTM standard D 2734, the void volume fraction was determined as:

$$\Phi_v = \frac{\rho_{th} - \rho_{comp}}{\rho_{th}} \tag{2}$$

where the theoretical density of the composite in absence of voids (ρ_{th}) was computed as:

$$\rho_{th} = \frac{1}{\frac{W_f}{\rho_f} + \frac{W_m}{\rho_m}} \tag{3}$$

where W_m and ρ_m are the matrix weight fraction and density, respectively.

Morphology of polished fracture surfaces of composite laminates was investigated by a Zeiss Axiophot optical microscope, equipped with a Leica DC300 digital camera, at a magnification of 500×.

2.2.2. Mechanical loading under ramp and creep conditions and electrical resistivity measurements

Quasi-static tensile tests and creep tests were performed at 25 °C on 250 mm long, 15 mm wide and 0.7 mm thick specimens, by using a MTS 858 Mini Bionix servo-hydraulic testing machine (Eden Prairie, Minnesota, USA), connected to a RT3 real-time digital control system by Trio Sistemi e Misure Srl (Bergamo, Italy). In order to keep the test temperature under control, all tests were carried out in Instron model 3119 thermostatic chamber (Norwood, Massachusetts, USA). The adopted testing configuration is documented in Fig. 1a. The monitoring of electrical resistance and of the temperature was performed through a 6½-digit electrometer/high resistance system model 6517A by Keithley Instruments Inc. (Cleveland, Ohio, USA). A voltage of 10 V was applied between two plastic clips covered by thin copper plates placed at a distance of 30 mm (Fig. 1b). The contact zones on the sample were painted with a silver electrical conductive coating. A zoom on the particular of the electrical contact connections is represented in Fig. 1c. The clips of the electrical connection were designed in such a way the pressure applied on the specimen was sufficiently high to ensure good electrical contact, but without constraining the specimen in correspondence of the clips. The thermocouple of the multimeter was placed into the thermostatic chamber in proximity of the specimen. The simultaneous acquisition of electrical resistance and temperature signals was carried out at a sampling rate of 10 Hz.

First of all, the time dependency of the electrical resistance of unloaded laminates at various temperatures was determined. Electrical resistance data acquired during tensile and creep tests were thus corrected so that the contribution of time dependent phenomena on the electrical resistance not dependent on the mechanical deformation/damage can be taken into account.

Monotonic tensile tests were carried out at a constant cross head speed of 2 mm min^{-1} in order to determine the most important tensile properties of the composite samples. Tensile tests were performed to estimate the elastic modulus of the composite samples and the strain was recorded through a MTS (Eden Prairie, Minnesota, USA) model no. 634.31F-24 extensometer with a gauge length of 20 mm, up to a deformation level of 1%. The piston displacement was also recorded and corrected in order to take into

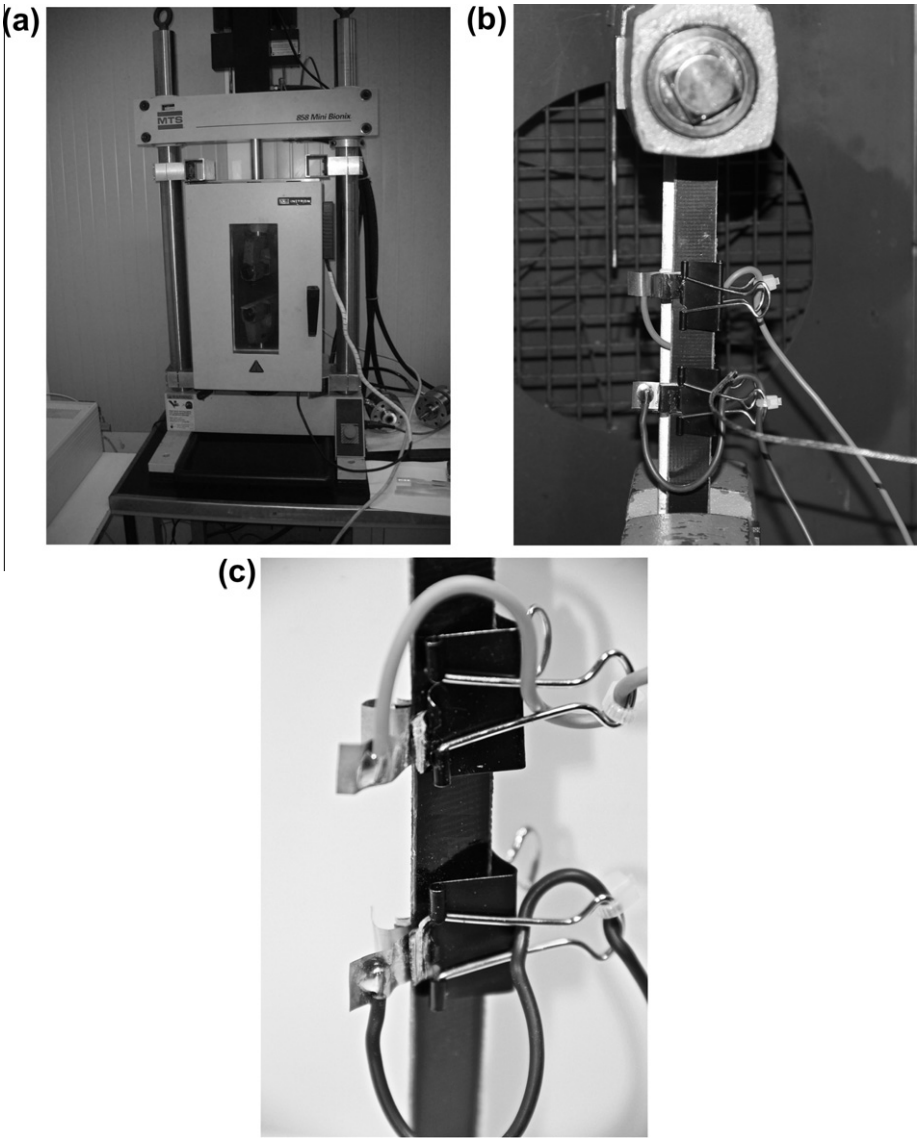

Fig. 1. Representative image of (a) the thermostatic chamber, of (b) experimental setup for the monitoring of the electrical conductivity and temperature during tensile mechanical tests under ramp and creep conditions, of (c) the electrical contact connections on the tested specimens.

account the machine compliance. According to ASTM D3039 standard, composite tabs were glued on the specimens extremities for a better clamping.

Creep tests were performed by using the same equipment on specimens of the same geometry at various stress levels (between 100 MPa and 350 MPa) in a temperature range between 20 and 90 °C, for a total loading time of 3600 s. Electrical resistance and temperature signals were acquired with a frequency of 1 Hz. A tensile creep compliance $D(t)$ was computed by dividing the time dependent strain $\varepsilon(t)$ by the constant applied stress σ_0. Due to the large deformation of the samples during the creep tests at high stresses or at elevated temperatures, the deformation was monitored normalizing the piston displacement for the gauge length of the samples (190 mm).

The capability of the tested materials to recover creep deformation was evaluated through recovery tests carried out both at room temperature and at 90 °C. In recovery tests, a constant stress of 300 MPa was applied for 1 h, and the deformation was monitored for 9 h after unloading.

3. Results and discussion

3.1. Thermal behavior and microstructural features of composites

The density of the tested laminates, the volumetric fraction of fibers and voids are reported in Table 1. Due to the presence of carbonaceous nanoparticles with a density higher than that of the neat matrix, Epoxy-CB/CNF-90/10-2-GF laminate shows a density higher than that of the composite with neat epoxy resin. The nanofilled composite presents also a higher void content with respect to the neat Epoxy-GF laminate. This could be probably related to the higher viscosity of the nanofilled resin. In fact, according to the literature information on the rheological behavior of nanofilled polymeric systems [31,32], the viscosity increase is mainly related to the polymer–filler and filler–filler interactions, depending on the nanofiller type and content. It can be therefore supposed that the degassing process during the preparation of the samples was less effective in the nanomodified laminates, with a consequent higher void content. Moreover, the fiber wetting capability of the matrix can be reduced by the viscosity increase induced by nanomodification [33]. Nevertheless, considering that the absolute values of void contents of the tested laminates is relatively small, their mechanical properties can be certainly compared.

Thermogravimetric curves of the Epoxy-GF and of the Epoxy-CB/CNF-90/10-2-GF specimens are reported in Fig. 2. The comparison of TGA curves of the two different specimens shows that the addition of nanofiller to the matrix does not remarkably affect the final residual mass.

In order to have information about the morphology of the investigated materials, micrographs of the polished surface of the tested specimens taken through the optical microscope are reported in Fig. 3. The quality of the micro-structural distribution of the fibers and impregnation were investigated by optical microscopy on the polished cross-section of laminates. As documented in Fig. 3, it can be observed that a good macro-impregnation is reached for both systems under investigation. The fiber volume fraction in

Table 1
Density, fiber volumetric fraction (ϕ_f), and void content (ϕ_v) of the two composite laminates.

	Epoxy-GF	Epoxy-CB/CNF-90/10-2-GF
Density (g cm^{-3})	1.925 ± 0.002	1.945 ± 0.002
ϕ_f (vol.%)	52.4	55.3
ϕ_v (vol.%)	1.0	2.1

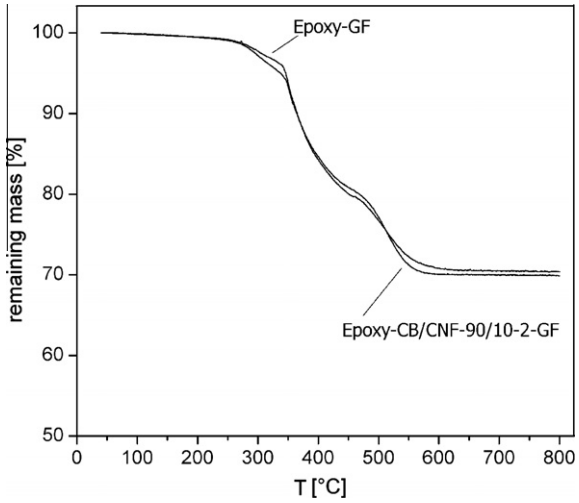

Fig. 2. TGA analysis performed on the Epoxy-GF sample and on the Epoxy-CB/CNF-90/10-2-GF sample.

Epoxy-GF and Epoxy-CB/CNF-90/10-2-GF samples were estimated by means of image analysis techniques (using Image J v.1.46a software), and fiber amounts of 61.2% ± 3.2% and 67.1% ± 4.8% were respectively determined. As reported in Table 1, fiber contents of 52.4% and 55.3% were calculated for the same samples through thermogravimetric analysis.

This discrepancy could be explained considering the relatively high statistical uncertainty of thermogravimetric tests for the

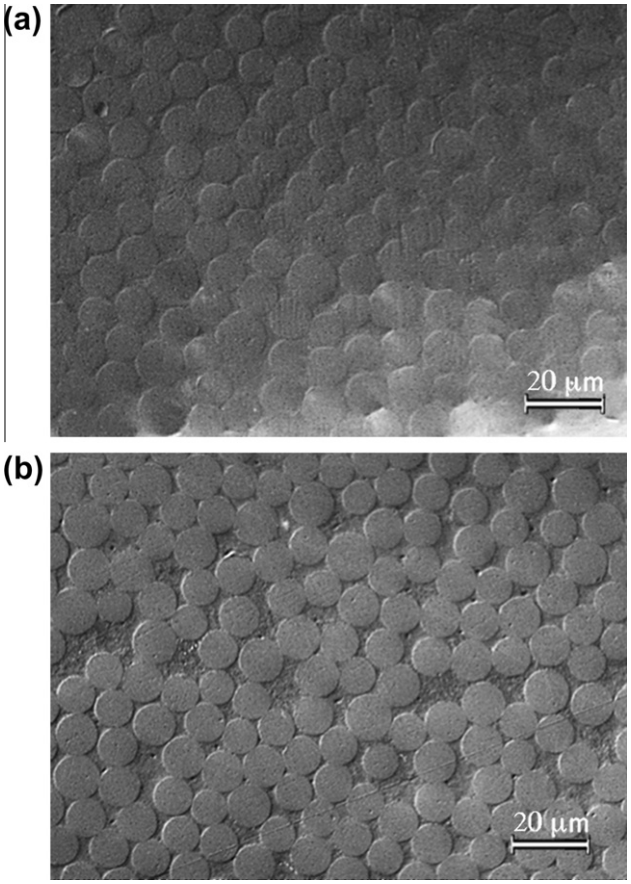

Fig. 3. Micrographs of the (a) Epoxy-GF and (b) Epoxy-CB/CNF-90/10-2-GF composites taken at the optic microscope at 500×.

evaluation of the fiber content. In this work only one measure was performed for each composition, but the result is affected by several factors such as the vacuum bagging during the manufacturing of the laminates and the position in the laminate from which the sample is taken.

3.2. Monitoring the mechanical response under ramp and creep conditions through electrical resistivity

In order to determine the influence of the nanomodification on the tensile properties of the tested laminates, quasi-static ramp tests were carried out on Epoxy-GF and Epoxy-CB/CNF-90/10-2-GF samples. As summarized in Table 2, the composite based on neat matrix exhibits similar tensile properties of that containing the nanomodified resin. As expected, the main contribution to the tensile properties of fiber reinforced laminates is given by the high volume fraction of continuous fibers. Therefore, the influence of the nanofiller on the longitudinal tensile properties of the composites is quite limited.

Stress–strain behavior and relative electrical resistance variation ($\Delta R/R_0$) during quasi-static tensile tests on Epoxy-CB/CNF-90/10-2-GF sample are reported in Fig. 4 (an initial electrical resistance of 11.58 ± 0.72 kΩ was measured before the load application). The $\Delta R/R_0$ curve follows a linear trend at low deformation ($\varepsilon < 1\%$), with a rapid increase of the slope when final failure is approached, probably due to a consistent damage evolution within the matrix. In particular it should be underlined the high sensitivity of the $\Delta R/R_0$ curve at low deformation levels, This result is even more significant if compared to those reported in similar works. In fact, Boeger et al. [27] and Nanni et al. [29] showed a quite low sensitivity of the electrical resistance at low deformation levels, with a significant delay with respect to the applied strain.

Therefore, this system seems to be particularly suitable for continuous monitoring under ramp conditions, both in the first stages of the tests and near the failure of the samples. According to literature data [27–29], the self-monitoring capability of the nanocomposite laminates under investigation could be associated with the presence of a conductive network of carbon particles inside the epoxy matrix. The progressive increase of the strain during tensile tests causes particles separation and progressive break-up of this network, with a consequent increase of electrical resistance. Approaching the final failure, the permanent separation between particles leads to a more rapid increase of $\Delta R/R_0$ values.

The creep compliance curves at room temperature and the associated variation of the relative resistance of the Epoxy-CB/CNF-90/10-2-GF sample are compared in Fig. 5a for different stress levels, while Fig. 5b–d report the same quantities measured at 40, 60 and 90 °C, respectively. The values of the initial resistances of the specimens tested under creep conditions are reported in Table 3.

The Epoxy-CB/CNF-90/10-2-GF sample exhibits primary and secondary creep behavior for an applied stress between 100 and 350 MPa at room temperature, 40 °C and 60 °C, while it shows a progressive increase of the creep rate till the failure (i.e. tertiary creep) for stresses higher than 300 MPa at 60 and 90 °C. A initial sudden increase of the electrical resistance upon load application can be observed for all samples, proportionally to the stress level. This is due to the strain induced by the elastic response of the material upon the instantaneous application of the load. It is interesting to note how $\Delta R/R_0$ tends to decrease with time at all the stress levels when the test is performed at room temperature and at 40 °C, while at 60 °C a flat plot can be detected for all creep stresses. $\Delta R/R_0$ plot evaluated at 90 °C tends to increase for creep stresses higher than 200 MPa, probably because the test temperature was close to the glass transition temperature of the system. As reported in a previous work [30], the glass transition temperature of the neat resin is 82 °C, and it increases until a nanofiller concentration of 1 wt.%, and then decreases for higher loadings. Therefore, for the Epoxy-CB/CNF-90/10 sample the same T_g value of the neat resin was determined. Creep tests performed at temperature slightly above the glass transition temperature (i.e. 90 °C) showed an increase of the relative resistance with respect to the deformation even after the instantaneous application of the load. According to some literature references [4], this results could be explained considering that, when a load is applied, the free volume between macromolecules is supposed to be higher in nanofilled samples with respect to the neat resin, with a correspondent decrease of their glass transition temperature [34]. Therefore, the lowering of the creep resistance due to the T_g drop in nanofilled specimens could be responsible of the observed increase of the electrical resistance.

The creep monitoring capability of the selected composite is therefore strongly affected by applied stress and temperature.

Different deformation and conduction mechanisms should be invoked to explain the creep behavior of the tested samples. It can be hypothesized that, as a consequence of the instantaneous application of the creep load, the conductive network within the polymer matrix is seriously damaged, with a consequent resistivity increase. When the kinetics of deformational processes is low (i.e. at low temperatures and/or at low stresses), nanoparticles are able to re-form a conductive network, thus inducing a progressive decrease of the electrical resistance with time. On the other hand, at elevated creep stresses and/or temperatures, the higher strain rate (i.e. rate of flow of material) may hinder the re-formation of the conductive path, with a progressive increase of $\Delta R/R_0$ values in time. However, this is only an hypothesis, and further investigations concerning tensile and creep tests at different temperatures

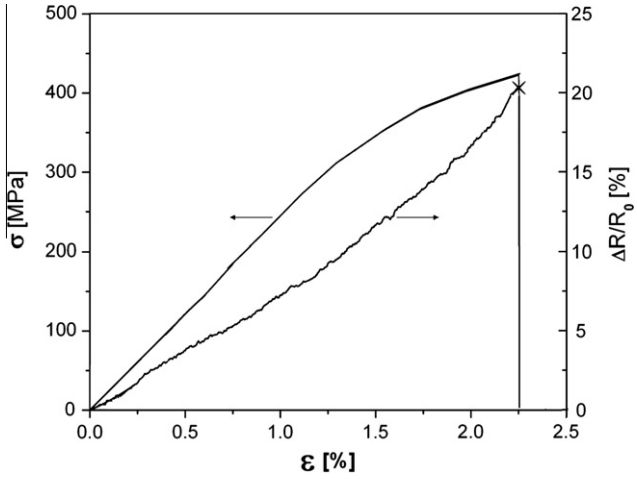

Fig. 4. Representative stress–strain and $\Delta R/R_0$ curves of the Epoxy-CB/CNF-90/10-2-GF sample during tensile mechanical test under ramp conditions (initial electrical resistance of 11.58 ± 0.72 kΩ).

Table 2
Quasi-static tensile mechanical properties of the Epoxy-GF and of the Epoxy-CB/CNF-90/10-2-GF composites.

	Epoxy-GF	Epoxy-CB/CNF-90/10-2-GF
E (GPa)	24.7 ± 1.3	25.4 ± 1.5
σ_b (MPa)	439 ± 12.5	445 ± 15.3
ε_b (%)	2.2 ± 0.2	2.3 ± 0.2

E: Elastic modulus.
σ_b: Ultimate tensile stress.
ε_b: Tensile strain at break.

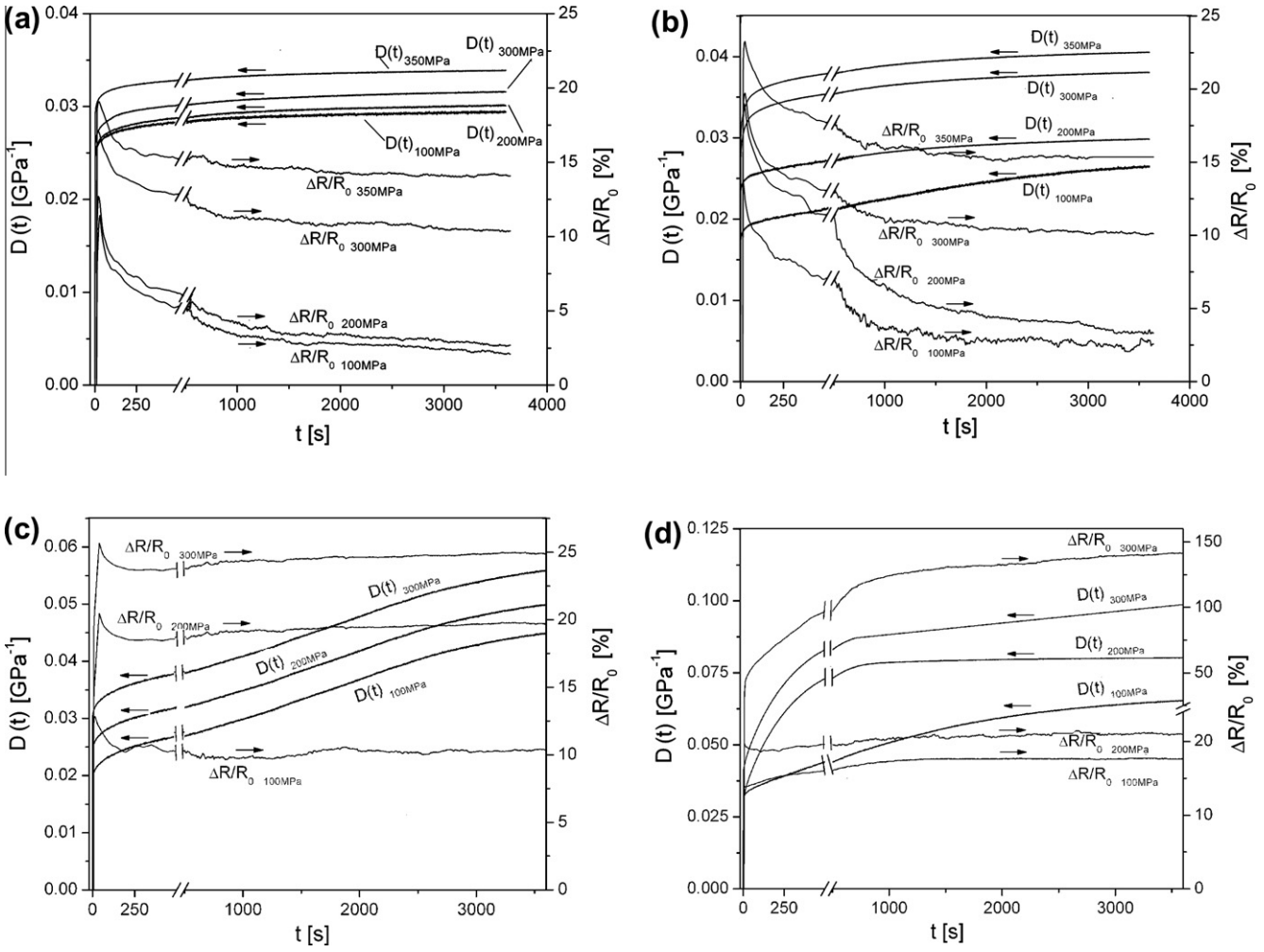

Fig. 5. Creep compliance and $\Delta R/R_0$ for different applied stresses of the Epoxy-CB/CNF-90/10-2-GF sample at (a) room temperature, (b) 40 °C, (c) 60 °C and (d) 90 °C.

Table 3
Initial resistance values (R_0) of the Epoxy-CB/CNF-90/10-2-GF samples before the application of the creep stress (σ_0).

Test	σ_0 (MPa)	T (°C)	R_0 (kΩ)
Creep	100–350	23	12.03 ± 1.13
Creep	100–350	40	11.22 ± 1.05
Creep	100–350	60	10.63 ± 1.16
Creep	100–300	90	10.84 ± 0.48
Creep and recovery	300	23	10.70
Creep and recovery	300	90	11.68

and/or strain rates are required for a better understanding of this phenomenon. However, regardless the dependency of $\Delta R/R_0$ trend from the testing temperature and/or stress, the variation of $\Delta R/R_0$ values with the creep time seems to be suitable for the monitoring of composite structures under constant loads. Even in this case the fluctuations of $\Delta R/R_0$ values due to external electromagnetic interferences are negligible with respect to the variations induce by the application of the load over the whole range of testing conditions.

In order to obtain a better correlation between electrical resistance and creep strain, in Fig. 6a and b the $\Delta R/R_0$ values are plotted as a function of the longitudinal deformation during creep tests performed at different stresses on the Epoxy-CB/CNF-90/10-2-GF sample at room temperature and at 90 °C, respectively. The initial resistance variation, due to the instantaneous application of the stress, follows a linear trend, decreasing its slope with the applied stress. After this stage, $\Delta R/R_0$ tends to decrease in time for all the creep stresses at room temperature. It is interesting to note that this decrease is more rapid when low creep loads are applied. This is probably due to the fact that when elevated stresses are applied, the re-formation of a conductive path within the sample is hindered by the elevated strain rate, and the decrease of $\Delta R/R_0$ is slower. Differently, the monitoring of the tests performed at 90 °C (Fig. 6b) shows that $\Delta R/R_0$ increases with the deformation even after the instantaneous application of the load. Even in this case it can be hypothesized that the re-formation of the filler network is hindered by the high strain rate experienced at elevated temperatures.

In order to investigate the potential of the selected system in monitoring the recovery of the deformation after unloading, some creep and recovery tests were also performed. In Fig. 7a the plots of the relative deformation and $\Delta R/R_0$ values versus time performed at room temperature and under an applied stress of 300 MPa are reported, while in Fig. 7b the plots of the corresponding tests carried out at 90 °C are represented. At room temperature, the sample is able to recover almost all the applied deformation after unloading, while a remarkable residual deformation remained at the end of the recovery stage for the test carried out at 90 °C. It is interesting to note how at room temperature the electrical resistance measured at the end of the recovery time is similar to the initial value, while at 90 °C the final resistance is remarkably higher than that registered at the beginning of the test. The permanent increase of the electrical resistance registered for the test performed at 90 °C

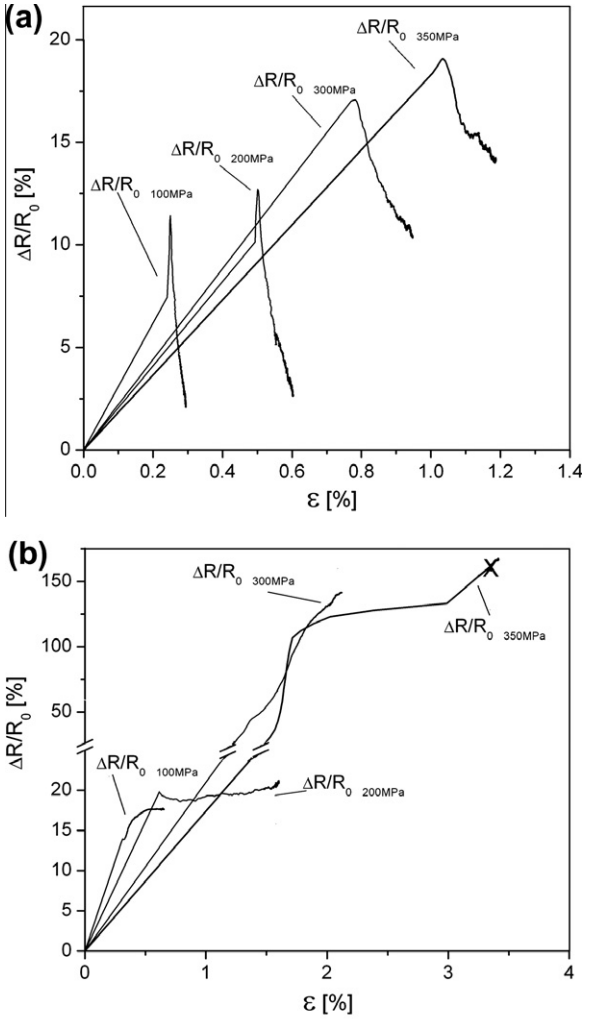

Fig. 6. $\Delta R/R_0$ vs longitudinal deformation during the creep tests performed on the Epoxy-CB/CNF-90/10-2-GF sample at (a) room temperature and (b) 90 °C.

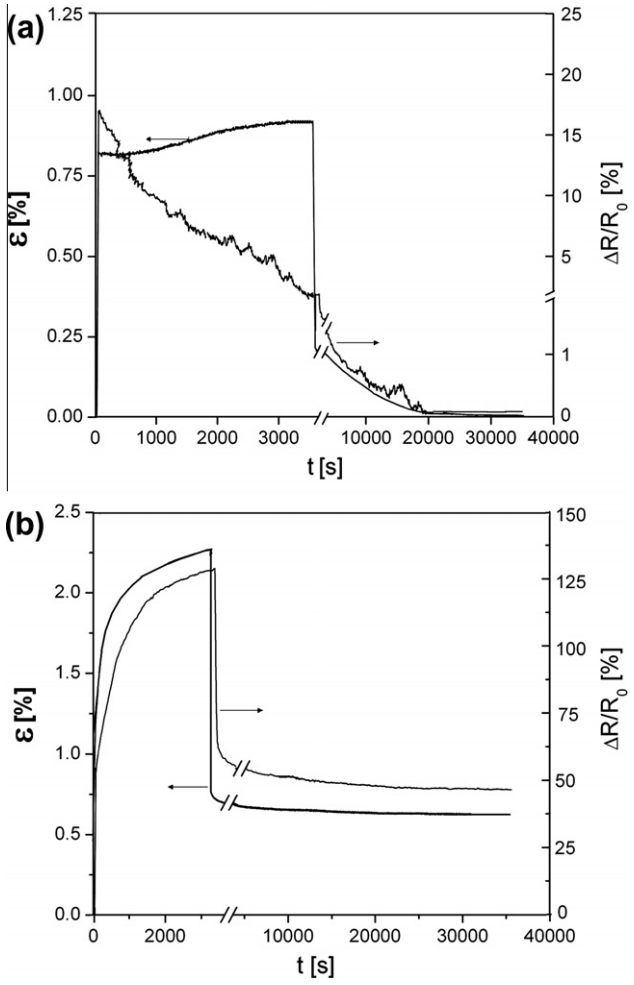

Fig. 7. Relative deformation and $\Delta R/R_0$ of the Epoxy-CB/CNF-90/10-2-GF sample for a creep test and following recovery performed at (a) room temperature and (b) 90 °C (applied creep stress of 300 MPa).

is evidently related to the permanent deformation and/or damage within the matrix accumulated during the loading stage. Therefore, it can be concluded that the investigated system shows promising monitoring capabilities also during the deformation recovery stage.

4. Conclusions

On the basis of the results of a previous work, an epoxy system containing a total nanofiller amount of 2 wt.%, with a relative CB/CNF ratio of 90/10 was selected for the preparation of glass fiber composite laminates, to be monitored under ramp and creep conditions. From quasi-static tensile tests, a direct correlation between tensile strain and the increase of the electrical resistance was observed, while in creep tests a more complex behavior, depending on the temperature and the applied stress, was detected. Creep and recovery tests showed that a complete recovery of the deformation was associated to a restoration of the monitored resistance till the initial values, while the residual deformation experienced at elevated temperature was related to a final electrical resistance 50% higher with respect to its initial value. Therefore, it was clearly demonstrated how the self monitoring of composite laminates through electrical resistance measurements could represent a promising way to evaluate their integrity under different loading and environmental conditions.

References

[1] Ashby MF. Material selection in mechanical design. Oxford: Elsevier; 2005.
[2] Staszewski WJ, Boller C, Tomlinson GR. Health monitoring of aerospace structures: smart sensor technologies and signal processing. Chichester (England): John Wiley and Sons Ltd.; 2004.
[3] Li C, Thostenson E, Chou T. Sensors and actuators based on carbon nanotubes and their composites: a review. Compos Sci Technol 2008;68(6):1227–49.
[4] Todoroki A. self-sensing of strain/damage of CFRP using electrical resistance changes. In: Proceedings of the XIth international congress and exposition. Orlando, Florida, USA: Society for Experimental Mechanics Inc.; 2008.
[5] Todoroki A, Ueda M, Hirano Y. Strain and damage monitoring of CFRP laminates by means of electrical resistance measurement. J Solid Mech Mater Eng 2007;1(8):947–74.
[6] Xia Z. Quantitative damage detection in CFRP composites coupled mechanical and electrical models. Compos Sci Technol 2003;63(10):1411–22.
[7] Lee DC, Lee JJ, Yun SJ. The mechanical characteristics of smart composite structures with embedded optical fiber sensors. Compos Struct 1995;32(1–4):39–50.
[8] Seo DC, Lee JJ. Effect of embedded optical fiber sensors on transverse crack spacing of smart composite structures. Compos Struct 1995;32:51–8.
[9] Dorigato A, Morandi S, Pegoretti A. Effect of nanoclay addition on the fibre/matrix adhesion in epoxy/glass composites. J Compos Mater; in press.
[10] Dorigato A, Pegoretti A. Development and thermo-mechanical behaviour of nanocomposite epoxy adhesives. Polyme Adv Technol 2012;23:660–8.
[11] Dorigato A, Pegoretti A. The role of alumina nanoparticles in epoxy adhesives. J Nanopart Res 2011;13:2429–41.
[12] Dorigato A, Pegoretti A, Bondioli F, Messori M. Improving epoxy adhesives with zirconia nanoparticles. Compos Interfaces 2010;17:873–92.
[13] Dorigato A, Pegoretti A, Quaresimin M. Thermo-mechanical characterization of epoxy/clay nanocomposites as matrices for carbon/nanoclay/epoxy laminates. Mater Sci Eng A 2011;528:6324–33.
[14] Isik I, Yilmazer U, Bayram G. Impact modified epoxy/montmorillonite nanocomposites: synthesis and characterization. Polymer 2003;44:6371–7.

[15] Liu W, Hoa SV, Pugh M. Fracture toughness and water uptake of high performance epoxy/nanoclay nanocomposites. Compos Sci Technol 2005;65:2364–73.
[16] Ragosta G, Abbate M, Musto P, Scarinzi G, Mascia L. Epoxy-silica particulate nanocomposites: chemical interactions, reinforcement and fracture toughness. Polymer 2005;46:10506–16.
[17] Varghese S, Gatos KG, Apostolov AA, Karger-Kocsis J. Morphology and mechanical properties of layered silicate reinforced natural and polyurethane rubber blends produced by latex compounding. J Appl Polym Sci 2004;92:543–51.
[18] Zhao C, Qin H, Gong F, Feng M, Zhang S, Yang M. Mechanical, thermal and flammability properties of polyethylene/clay nanocomposites. Polym Degrad Stab 2005;87(1):183–9.
[19] Fan ZJ, Zheng C, Wei T, Zhang YC, Luo GL. Effect of carbon black on electrical property of graphite nanoplatelets/epoxy resin composites. Polym Eng Sci 2009;49(10):2041–5.
[20] Kumar S, Sun LL, Caceres S, Li B, Wood W, Perugini A, et al. Dynamic synergy of graphitic nanoplatelets and multi-walled carbon nanotubes in polyetherimide nanocomposites. Nanotechnology 2010;21(10).
[21] Lee JH, Jang YK, Hong CE, Kim NH, Li P, Lee HK. Effect of carbon fillers on properties of polymer composite bipolar plates of fuel cells. J Power Sources 2009;193(2):523–9.
[22] Li J, Wong PS, Kim JK. Hybrid nanocomposites containing carbon nanotubes and graphite nanoplatelets. Mater Sci Eng A Struct Mater Properties Microstruct Proc 2008;483–484(SI):660–3.
[23] Ma PC, Liu MY, Zhang H, Wang SQ, Wang R, Wang K, et al. Enhanced electrical conductivity of nanocomposites containing hybrid fillers of carbon nanotubes and carbon black. ACS Appl Mater Interfaces 2009;1(5):1090–6.
[24] Sumfleth J, Buschhorn ST, Schulte K. Comparison of rheological and electrical percolation phenomena in carbon black and carbon nanotube filled epoxy polymers. J Mater Sci 2010;46(3):659–69.
[25] Traina M, Pegoretti A, Penati A. Time-temperature dependence of the electrical resistivity of high-density polyethylene/carbon black composites. J Appl Polym Sci 2007;106(3):2065–74.
[26] Thostenson ET, Chou TW. Carbon nanotube networks: sensing of distributed strain and damage for life prediction and self healing. Adv Mater 2006;18(21):2837–41.
[27] Boeger L, Wichmann MHG, Meyer LO, Schulte K. Load and health monitoring in glass fibre reinforced composites with an electrically conductive nanocomposite epoxy matrix. Compos Sci Technol 2008;68(7–8):1886–94.
[28] Kostopoulos V, Vavouliotis A, Loutas T, Karapappas P. Multi-stage fatigue life monitoring on quasi-isotropic carbon fibre reinforced polymers enhanced with multi-wall carbon nanotubes: Parallel use of electrical resistance, acoustic emission, and acoustoultrasonic techniques. In: Nondestructive characterization for composite materials, aerospace engineering, civil infrastructure, and homeland security. San Diego, CA; 2009.
[29] Nanni F, Ruscito G, Puglia D, Terenzi A, Kenny JM, Gusmano G. Effect of carbon black nanoparticle intrinsic properties on the self-monitoring performance of glass fibre reinforced composite rods. Compos Sci Technol 2010:20.
[30] Pedrazzoli D, Dorigato A, Pegoretti A. Monitoring the mechanical behaviour under ramp and creep conditions of electrically conductive polymer nanocomposites. J Nanosci Nanotechnol; in press.
[31] Cassagnau P. Melt rheology of organoclay and fumed silica nanocomposites. Polymer 2008;49:2183–96.
[32] Dorigato A, Pegoretti A, Penati A. Linear low-density polyethylene – silica micro- and nanocomposites: dynamic rheological measurements and modeling express. Polymer Letters. 2010;4(2):115–29.
[33] Lee SM. Handbook of composite reinforcements. Palo Alto: Wiley-VCH; 1993.
[34] Haward RN, Young RJ. The physics of glassy polymers. London: Chapman & Hall; 1997.